Published in "Journal of Geophysical Research (2010): F01014"
which should be cited to refer to this work.

Combined observations of rock mass movements using satellite SAR interferometry, differential GPS, airborne digital photogrammetry, and airborne photography interpretation

Tazio Strozzi,[1] Reynald Delaloye,[2] Andreas Kääb,[3] Christian Ambrosi,[4] Eric Perruchoud,[2] and Urs Wegmüller[1]

[1] Recent global warming, through the related retreat of mountain glaciers, causes a growing number of different slope instabilities requiring accurate and cost-effective monitoring. We investigate the potential of combined remote sensing observations from satellite and airborne microwave and optical sensors for an efficient survey of mountainous ground displacements. The evolution of a paraglacial deep-seated rock mass movement due to glacier retreat in the Swiss Alps has been observed between 1976 and 2008 with satellite synthetic aperture radar (SAR) interferometry, differential GPS, and airborne digital photogrammetry. Analysis of differential SAR interferograms revealed an acceleration of the landslide from ~4 cm/yr in the slope-parallel direction during the mid-1990s to more than 30 cm/yr in the summer of 2008. Differential GPS surveys performed between the summers of 2007 and 2008 indicate seasonal variations of the landslide activity. The photogrammetric analysis revealed no significant movement (i.e., <1 cm/yr) between 1976 and 1995 and provides an overview of the total displacement between 1995 and 2006 with high spatial resolution. In situ and airborne photography interpretation suggests that the landslide was activated at earliest by the end of the Last Glaciation but without any significant long-lasting activity during the Holocene and that the exponentially increasing reactivation since the 1990s is the result of ongoing debutressing of the valley flank due to the glacier retreat in combination with strong precipitation and snowmelt events. We conclude that the employed remote sensing techniques complement each other well within a landslide hazard assessment procedure.

1. Introduction

[2] Recent atmospheric warming causes significant shrinking of glaciers for most mountain regions around the world [*Zemp et al.*, 2008]. The pronounced retreat of valley glaciers leads, in particular, to ice volume losses in the terminus sections [e.g., *Paul et al.*, 2004; *Paul and Haeberli*, 2008]. The related changes of the stress regime of the adjacent valley flanks may under certain geological conditions cause a number of types of landslides, not least deep-seated rock mass movements [*Blair*, 1994; *Ballantyne*, 2002; *Matsuoka and Masahiro*, 2002; *Kääb*, 2005; *Kääb et al.*, 2005]. In Switzerland the decline of alpine glaciers has been observed since the end of the Little Ice Age (LIA, circa 1850) with an acceleration phase since the 1980s. The Great Aletsch Glacier in the Canton of Valais, with its current length of ~23 km, its surface of ~86 km^2, and its maximum depth of ~900 m the largest stream of ice in the European Alps, retreated horizontally by 2785 m from 1870 to 2007 (Swiss Glacier Monitoring Network, http://glaciology.ethz.ch/messnetz, accessed 15 March 2009). At the current terminus position at ~1700 m above sea level (asl), Great Aletsch Glacier lost ~200 m in ice thickness between 1850 and 1976 (−1.5 m/yr), 50 m between 1976 and 1995 (−2.5 m/yr), and 60 m between 1995 and 2006 (−6 m/yr). Because of the geological and terrain conditions found at the slopes adjacent to the tongue of Great Aletsch Glacier, a number of rock mass movements are currently active, and the area appears as a natural laboratory for investigating such types of slope instabilities.

[3] On the left side of Great Aletsch Glacier between Riederfurka and Bettmerhorn, a large unstable rock mass

[1]Gamma Remote Sensing, Gümligen, Switzerland.
[2]Geography Unit, Department of Geosciences, University of Fribourg, Fribourg, Switzerland.
[3]Department of Geosciences, University of Oslo, Oslo, Norway.
[4]Institute of Earth Sciences, University of Applied Sciences of Southern Switzerland, Canobbio, Switzerland.

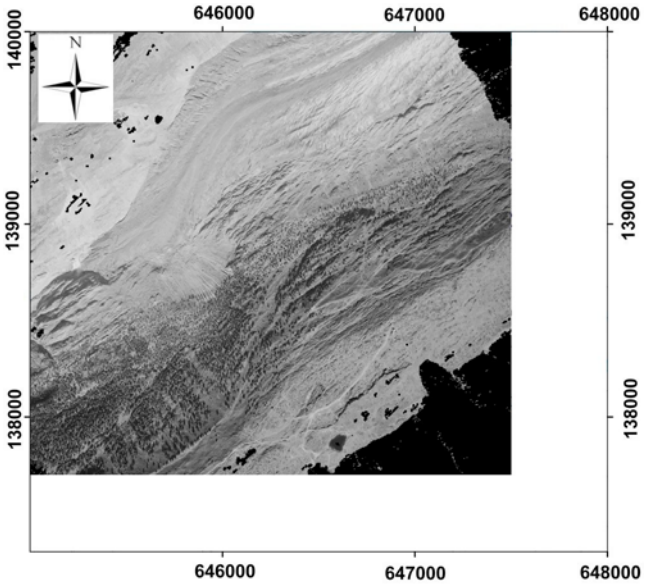

Figure 1. Aerial photography of the Aletschwald landslide of 5 September 2006.

was detected with the use of ERS differential synthetic aperture radar (SAR) interferometry [*Strozzi et al.*, 2002]. The displacement was visible between 1992 and 1998 in annual interferograms and in 105 days in the summer of 1999. As later confirmed with JERS SAR data [*Strozzi et al.*, 2003], the landslide was affecting an area of more than 1 km^2 from the glacier margin up to the top of the ridge. More recent Advanced Land Observing Satellite (ALOS) Phased Array type L-band Synthetic Aperture Radar (PALSAR) and Envisat advanced synthetic aperture radar (ASAR) interferograms of 2006 and 2007 revealed an important acceleration of the landslide from a few cm/yr at the beginning of the observation period to a few cm/month at present [*Strozzi et al.*, 2007]. In order to endorse these results and to obtain additional information on the landslide kinematic, we suggest complementing differential SAR interferometry with other remote sensing and in situ techniques [*Kääb*, 2005; *Brückl et al.*, 2006; *Delacourt et al.*, 2007]. Therefore, we designed a network of GPS points and repeated measurements four times between the summers of 2007 and 2008. In parallel, we photogrammetrically analyzed airborne photographs taken over Great Aletsch Glacier at the end of the summers of 1976, 1995, and 2006.

[4] In this contribution we compare and discuss in detail the various remote sensing methods employed for the survey of the unstable slope above the tongue of Great Aletsch Glacier, we present the measurement results in order to understand the accelerating slope movement in response to the glacier retreat, and we draw general conclusions for hazard management in alpine regions. Such rock slides increasingly present problems to mountain infrastructure and landscape. In our region of interest, for instance, not only is the massive glacier unique but also the forest at the glacier's edge with the tongue of Great Aletsch Glacier reaching far below the regional timber line. In particular, the area above the LIA lateral moraine is dominated by a developed stock of pines and larches with dense undergrowth made of cotton grass and dwarf shrubs. Tests have shown that the pines in the Aletsch forest (local name Aletschwald) are at least 600–700 years old (Pro Natura Center Aletsch, http://www.pronatura.ch/aletsch, accessed 15 March 2009). In 1933, the entire area was put under absolute protection by Pro Natura, Switzerland's nature conservation organization, and since 2001 it has been inscribed in the UNESCO World Heritage List (UNESCO World Heritage Centre, http://whc.unesco.org, accessed 15 March 2009). Ever since, 50,000–70,000 visitors admire the 410 ha of the protected area every year, also using a cableway that is situated in its upper section on the sliding area. An efficient survey of the unstable slopes in this region is thus of particular interest and will be of even increasing importance in the future.

2. Methods

2.1. Airborne Photography Interpretation

[5] The interpretation of optical images is commonly applied in support of landslide mapping and inventories. In Switzerland, airborne photographs are regularly acquired for topographic mapping and map update at ~1:20,000 scale. On the basis of the interpretation of stereoscopic aerial photographs complemented by topographic maps, Digital Elevation Models (DEMs), field surveys, and historical records, sketch maps of landslides can be produced. Landslides are usually discriminated by typology, depth, and activity. In particular, a distinction between rotational and translational slides, complex slides and rockfalls, deep-seated gravitational slopes, and diffuse shallow slides can be achieved. The high resolution of aerial photographs also permits us to recognize geomorphological features associated with mass movements, such as scarps, counterscarps, trenches, debris flows, debris fans, and rockfalls.

[6] For the Aletschwald landslide the stereoscopic aerial photographs considered for airborne photography interpretation were taken on 5 September 2006 (see Figure 1). Great Aletsch Glacier is visible in the central upper part of Figure 1, flowing approximately toward southwest and terminating at the central left part of Figure 1. The complex geomorphology of the area under investigation on the left side of Great Aletsch Glacier is evident, with a series of moraines scarps and counterscarps. Forest is covering, in particular, the southwestern part of the slope.

2.2. Satellite SAR Interferometry

[7] Spaceborne SAR systems offer the possibility to survey large areas, even in remote locations. Repeat-pass differential SAR interferometry (InSAR) is a powerful technique for mapping land surface deformation from space at fine spatial resolution [*Bamler and Hartl*, 1998; *Rosen et al.*, 2000; *Strozzi et al.*, 2001; *Catani et al.*, 2005]. InSAR makes use of two SAR images acquired from slightly different orbit configurations and at different times to exploit the phase difference of the signals. The phase signal derived from an image pair relates both to topography and line-of-sight surface movement occurring between the acquisitions, with atmospheric phase distortions, signal noise, and inaccuracy in the orbit determination as main error sources. In differential InSAR the topography-related phase is subtracted from the interferogram to derive a displacement map.

Table 1. Sensors, Acquisition Dates, Time Differences, and Perpendicular Baselines of the Selected SAR Interferograms

SARSensor	Acquisition Dates	Time Interval (days)	Perpendicular Baseline (m)
ERS	6 Oct 1992 to 21 Sep 1993	350	−44
ERS	8 Jun 1993 to 6 Jul 1995	758	39
JERS	17 Jun 1993 to 4 Aug 1996	1144	45
ERS	11 Aug 1995 to 26 Jul 1996	350	121
ERS	11 Aug 1995 to 15 Aug 1997	735	35
ERS	26 Jul 1996 to 15 Aug 1997	385	−86
ERS	15 Aug 1997 to 4 Sep 1998	385	−53
ERS	9 Oct 1998 to 16 Jul 1999	280	−126
ERS	16 Jul 1999 to 29 Oct 1999	105	7
ERS	13 Sep 2002 to 29 Aug 2003	350	64
ERS	29 Aug 2003 to 9 Jul 2004	315	−69
Envisat	22 Oct 2004 to 24 Jun 2005	245	21
Envisat	2 Sep 2005 to 14 Jul 2006	315	87
Envisat	9 Jun 2006 to 27 Oct 2006	140	−27
ALOS	13 Jun 2006 to 29 Oct 2006	138	−496
Envisat	29 Jun 2007 to 3 Aug 2007	35	1
Envisat	22 Aug 2007 to 31 Oct 2007	70	10
Envisat	6 Aug 2008 to 15 Oct 2008	70	−211
TerraSAR-X	22 Aug 2008 to 13 Sep 2008	22	−21

[8] The potential and limitations of InSAR for the periodical survey of alpine displacements were investigated by *Strozzi et al.* [2002, 2004] and *Delaloye et al.* [2007]. For the alpine territory, which is characterized by low or even absent vegetation, differential InSAR shows a relatively high coherence during the snow-free season between early summer and mid-fall, permitting the detection and monitoring of unstable slopes on a regular basis. Restrictions to the spatial coverage arise from decorrelation over forested and snow-covered areas and from layover and shadowing caused by the very rugged topography. In addition, the technique is better suited for the monitoring of the displacement of slopes facing away from the SAR look vector.

[9] In this study, we analyzed a series of SAR images from the European Remote Sensing satellites ERS-1, ERS-2, and Envisat, the Japanese Earth-Observation satellites JERS-1 and ALOS, and the German TerraSAR-X mission from 1992 to 2008. A total of 19 interferograms with short baselines and acquisition time intervals between 22 and 1144 days were considered (see Table 1). For topographic reference and orthorectification an external DEM with a pixel spacing of 25 m was used. The baseline was first estimated from the orbit data and subsequently refined on the basis of the fringe rate in range and azimuth directions. For the quantitative measurement of the identified displacement, phase unwrapping (i.e., the process to resolve the module 2π ambiguity of the interferometric phase) was performed after adaptive filtering [*Goldstein and Werner*, 1997], applying a region-growing algorithm [*Werner et al.*, 2002]. Phase unwrapping of interferograms in rugged terrain is a critical task that was successful only for small areas, depending also on the time period and wavelength of the interferograms. The line-of-sight displacement was finally transformed to displacement along the elevation gradient using the DEM.

[10] From the different error sources of InSAR (atmospheric phase distortions, signal noise, inaccuracy in the orbit determination, phase unwrapping mistakes, and assumption of displacement along the elevation gradient), we consider signal noise and assumption of displacement along the elevation gradient as the main limiting factors for the proposed application. The analyzed rock mass movement has a relatively small dimension of ~1 km^2, whereas atmospheric artifacts and inaccuracy in the orbit determination mainly cause relatively large scale distortions. Phase unwrapping was carefully performed with a region-growing algorithm, and only areas with reliable information were retained. To prevent errors caused by the transformation of the line-of-sight displacement along the elevation gradient, only measurements of slope with an orientation within 80° of the line of sight are presented. Assuming a total phase error of one quarter of wavelength leads to an error in line-of-sight displacement of 0.7 cm for ERS-1/2 and Envisat and of 0.4 cm for TerraSAR-X. This value is in agreement with the outcomes of a major InSAR validation project with average RMS errors of single ERS-1/2 and Envisat measurements ranging between 4 and 6 mm [*Crosetto et al.*, 2008]. For JERS and ALOS the assumed total phase error is minor [*Sandwell et al.*, 2008], for example, one eighth of wavelength, leading to an error in line-of-sight displacement of 1.5 cm.

2.3. Differential GPS

[11] Differential GPS (DGPS) makes use of two receivers in order to improve the accuracy of single measurements that are disturbed by the atmosphere. A reference receiver, set up at a fixed location that is assumed to be motionless, receives in permanence the satellite signals, calculates its position, and determines the difference with the coordinates attributed to its own position. A second receiver, called the rover, is mobile and placed successively on the points that need to be positioned. In real-time kinematic mode [*Lambiel and Delaloye*, 2004] the two receivers, reference and rover, are in a permanent state of communication, and the correction values are directly sent by radio from the reference to the rover. The main advantage of this mode in comparison to the triangulation technique is that visibility between the stations is not necessary. Therefore, it is not required to move the reference station once it is installed, but the topographic horizon can drastically limit the number of available satellites in a certain area. This technique allows a rapid acquisition of data once marking of points has been performed during the first campaign. In order to gain control of the measurement accuracy, the receiver is left calculating its position for ~10 s, and the average value of five to ten measurements is retained. The standard deviation of positioning during this time lapse is usually less than 1 cm in the horizontal component and less than 2 cm in the vertical one. By adding the positioning error, a total error up to 3 cm can be reached when comparing two sets of data.

[12] We marked a set of 45 points along hiking trails inside and outside the Aletschwald landslide area. The reference station and four control points are located outside the landslide and are assumed to be stationary. Trees and a closed horizon disturbed locally the reception of GPS signals. However, despite some waiting for better satellite constellations, most of the landslide can be surveyed within a few hours of fieldwork. Since September 2007 we repeatedly surveyed the 45 GPS points (see Table 2). It has to be noted that in May 2008, snow cover prevented measurements at a certain number of locations.

Table 2. Acquisition Dates and Time Differences of the GPS Surveys

Acquisition Dates	Time Interval (days)
5 Sep 2007 to 17 Oct 2007	42
17 Oct 2007 to 27 May 2008[a]	223
27 May 2008 to 6 Oct 2008[a]	132
17 Oct 2007 to 6 Oct 2008	355

[a]Indicates an incomplete series.

2.4. Airborne Digital Photogrammetry

[13] As demonstrated by earlier studies [*Kääb and Vollmer*, 2000; *Kaufmann and Ladstädter*, 2000; *Kaab*, 2002], digital photogrammetry based on repeated aerial photography (ADP) represents a suitable remote sensing tool for long-term monitoring of low deformation rates of a few cm/yr over wide areas. Here, multitemporal DEMs with 5 m grid spacing and orthoimages with 0.2 m spatial resolution were automatically computed from airborne photograph pairs of ~1:20,000 scale scanned at 14 μm. The overlapping image pairs were taken on 6 October 1975, 2 October 1995, and 5 September 2006 by the Swiss Federal Office of Topography (see Table 3). As a special measure to reduce geometric distortions between the image pairs, which could falsify the photogrammetric displacement measurements, we combined all images as one multitemporal image block and introduced multitemporal tie points [*Kääb and Vollmer*, 2000]. It was a significant problem during the image orientation in this study that large parts of the terrain covered by the airborne photographs used was changing or instable between the image acquisitions, such as the glacier or the rock mass movement under investigation. Multitemporal tie points had to be avoided over these terrain sections. In fact, several of the ground control points used turned out to be moving as indicated by the statistical error detection procedures during the photogrammetric adjustment. These points were iteratively excluded from the sensor model calculations until an accuracy of 0.4 m RMS was reached as the average error of the exterior orientation.

[14] Horizontal surface displacements were derived from automatic cross correlation of two subsequent orthoimages from different times. The software used for that purpose [*Kääb and Vollmer*, 2000] calculates the terrain displacement from gray value matching between multitemporal orthoimages. Validations of the procedure, for instance over stable terrain, revealed an accuracy for individual displacements on the order of 1 pixel, including also uncertainties resulting from the terrain itself, such as tilting rocks and forest cover. In our case, the applied orthoimages have a resolution of 20 cm in ground scale. This absolute accuracy translates into an accuracy for the velocity of ± 1 cm/yr RMS for the investigated 19 year period between 1976 and 1995, of ± 1.8 cm/yr RMS for the investigated 11 year period between 1995 and 2006, and of ± 0.7 cm/yr RMS for the entire 30 year period between 1976 and 2006. For the periods 1976–1995, 1995–2006, and 1976–2006, we computed matches at 10 m grid spacing.

Table 3. Acquisition Dates and Time Differences of the Aerial Photography Used for the Digital Photogrammetry Measurements

Acquisition Dates	Time Interval (days)
6 Sep 1976 to 2 Oct 1995	6965
2 Oct 1995 to 5 Sep 2006	3991

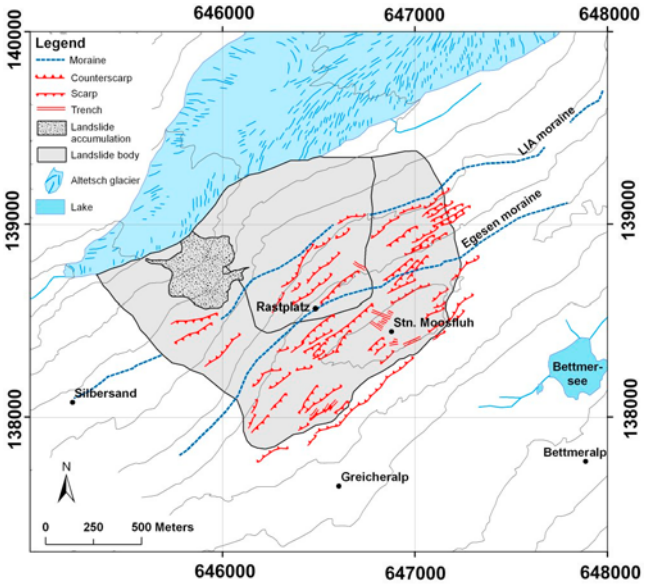

Figure 2. Sketch map of the Aletschwald landslide from the interpretation of the aerial photography of 5 September 2006. Contour lines are shown at 100 m height difference, and Station Moosfluh is at 2333 m above sea level.

3. Results

3.1. Airborne Photography Interpretation

[15] The sketch map of the Aletschwald landslide from aerial photography interpretation is presented in Figure 2. The image background represents selected topographic features with a grid size of 1 km.

[16] From the geological point of view the Aletschwald region belongs to the crystalline Aar massif and in particular to its old basis formed by migmatics gneiss [*Crisinel*, 1978]. The schistosity of the rocks is well defined with a northeast direction and a subvertical dip. The Great Aletsch Glacier is responsible for the morphology of the Aletschwald slope. The retreat of Great Aletsch Glacier, marked by a series of lateral moraines, caused the development of sometimes spectacular landslides. Close to the glacier, some relatively small landslides are visibly active. The most evident one, not indicated in Figure 2 but partly visible in Figure 1, is located below Silbersand and has a scar marked by a steep cliff of ~50 m height. Some morainic crests dating from the years 1912–1915 are slightly dislocated, indicating that this landslide is recent [*Crisinel*, 1978]. Another small landslide, indicated in Figure 2 as a pointed area, is more recent.

[17] The landslide affecting a large part of the Aletschwald region, indicated as a light gray area in Figure 2, is more ancient and is believed to be deep seated. The most evident sign of movement is the scarp in the upper part of the slope southeast of Station Moosfluh that shows several meters of displacement toward northwest. Scarps, counterscarps, and grabens occur in the upper part of ridge. These features range from a few meters to hundreds of meters in length, are 1–5 m high, and trend northwest, mostly parallel to the

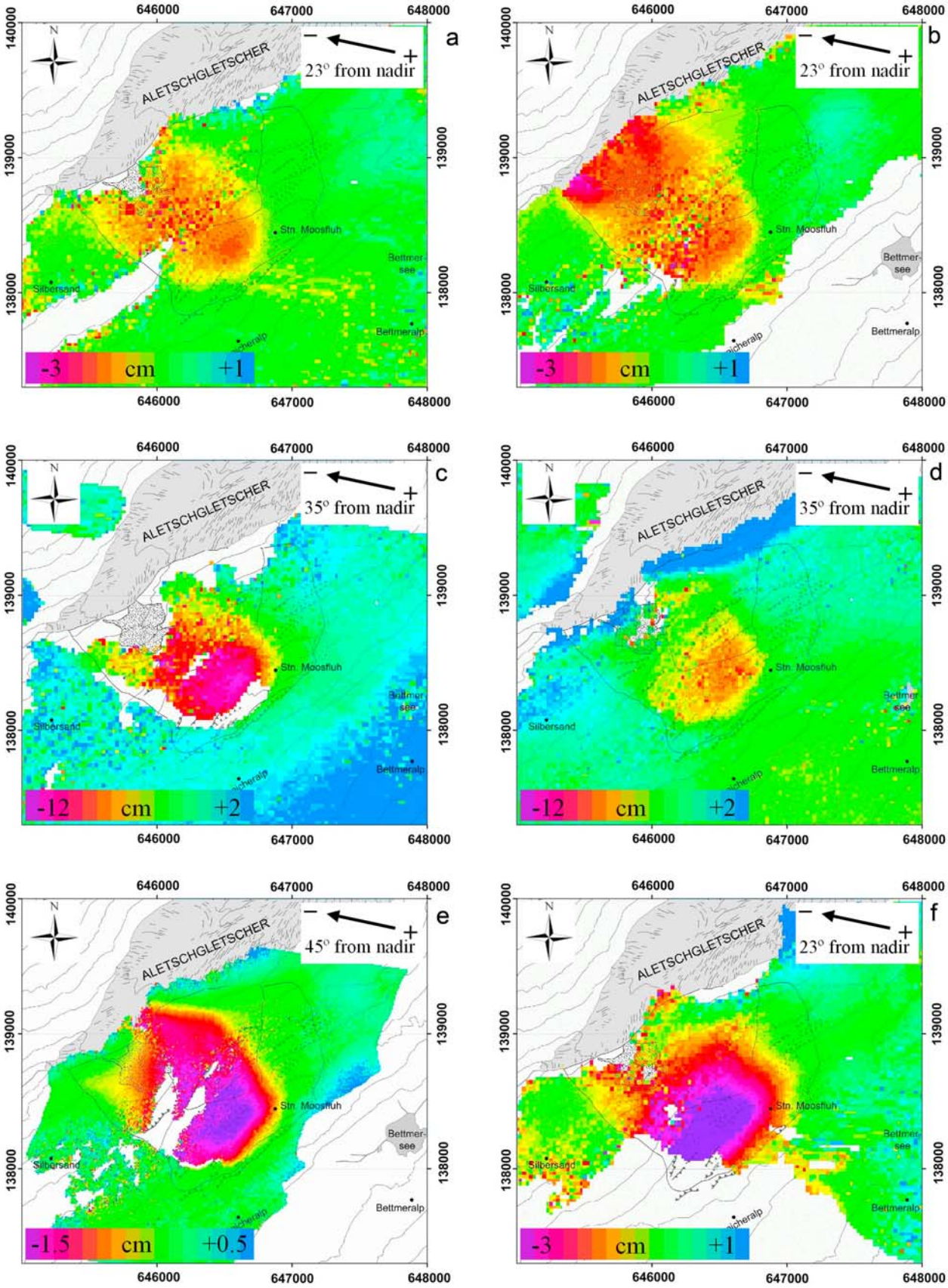

Figure 3

direction of the Great Aletsch glacier valley. Counterscarps reveal the activity of deep subvertical faults by the end of the Last Glaciation (known as the Würmian Glaciation in the European Alps), that is, postglacial rebound [*Ustaszewski et al.*, 2008]. In the middle and lower part of the slope, below Rastplatz, the landslide is barely visible on the topography, possibly because morphological evidence associated with the displacement is masked by moraines and sparse forest is largely covering the area. However, the displacement of the rocks has not been really significant. The lateral limits of the landslide are also difficult to distinguish and only discernible with the extended coverage of structures associated with the slope movements (scarps and counterscarps).

[18] Also shown in Figure 2 is the LIA lateral moraine, which represents the glacier position by circa 1860 when the glacier was ~3 km longer and 300 m higher than today. The LIA lateral moraine, which corresponds to the glacier maximal position during the Holocene, that is, approximately the last 10,000 years, is visible by a distinctive broad line of lighter material. Those light lines house some rather young vegetation, which has formed only over the past several decades.

[19] The maximum extent of the Last Glaciation occurred at ~18,000 years before present (B.P.). Deglaciation on the Alpine forelands occurred rapidly but with fluctuations apparent as a series of glacial advances [*Kelly et al.*, 2004]. In particular, prior to the early Holocene warming at ~10,000 years B.P., severe cold conditions returned to the Northern Hemisphere. At that time, the Younger Dryas cold period, Great Aletsch Glacier expanded considerably. The snout of the glacier laid in the Rhone valley, and its edge reached almost up to Moosfluh. At that time, the glacier developed a well-defined lateral moraine, the so-called Egesen moraine, which is still visible today in the Aletsch forest and is attesting the maximal glacier position by the end of the late glacial epoch [*Kelly et al.*, 2004].

[20] By the Last Glacial Maximum and during most of the late glacial epoch before the Younger Dryas, the glacier was overriding the Moosfluh ridge. Only the highest peaks rose above the massive expanse of ice. The glacially eroded surface by Moosfluh is no more intact, which means that the landslide was already activated by the end of the Last Glaciation. The geological structure is obviously tilted by ~25° to the northwest, essentially following the glacier direction. Because there is still no direct visible sign of the ongoing reactivation of the landslide when visiting the area and because the Egesen moraine is continuous across the moving area, it can be also concluded that the landslide was already activated before the Younger Dryas and that there has been no significant long-lasting activity during the Holocene.

3.2. Satellite SAR Interferometry

[21] Six out of the 19 displacement maps of the unstable slope in the Aletschwald region determined with InSAR are shown in Figure 3. Displacement maps for different SAR sensors, time periods, and acquisition time intervals are presented. The displacement is in the line-of-sight direction, and the negative sign indicates the direction away from the satellite. From 1992 to 1993 the displacement rate in a ERS-1 SAR interferogram was ~2 cm/yr in the center of the landslide (Figure 3a). In the summer of 2007 the signal related to the displacement of the landslide was visible in a 35 day time interval Envisat interferogram (Figure 3b), which indicates a displacement rate on the order of 1 cm/month or 15 cm/yr. A similar increase of the displacement rate was also observed on L-band SAR interferograms [*Strozzi et al.*, 2005]. In the three years between 1993 and 1996 a JERS SAR interferogram shows ~12 cm of displacement (Figure 3c). In 139 days during the summer of 2006 an ALOS PALSAR interferogram revealed a displacement of ~5 cm (Figure 3d).

[22] The deep-seated movement of the rock mass can be delimited from the differential SAR interferograms as a fairly consistent unit affecting an area of more than 1 km^2. The displacement rate is higher at the center of the landslide and is generally decreasing downslope. The border of the moving area is particularly well defined to the southwest of the slope, not only on the SAR interferograms but also in the landscape. Toward the top of the slope the limit of the landslide is mainly evident with the TerraSAR-X interferogram (Figure 3e). TerraSAR-X operates at X-band with an 11 day repeat cycle, and the SAR images considered in this study were acquired at ~3 m ground resolution in contrast to the ground resolution on the order of 20 m of the other SAR sensors. Toward northeast, the limit of the landslide is less obvious. With increasing time interval, for example, 1 year in ERS (Figure 3f), the area affected by discernible movement in the InSAR maps increases.

3.3. Differential GPS

[23] The differential GPS measurements of the Aletschwald landslide from 17 October 2007 to 6 October 2008 are presented in Figure 4. The blue lines represent the horizontal component of the motion, while the white lines represent the vertical component. The direction of movement is generally downsloping, and for most surveyed points there is only a small vertical component in the observed total motion. Because, in general, in the upper part of a landslide a larger subsidence rate can be expected, it seems that the deep-seated landslide is producing a tilting of the geological structure closer to the surface.

[24] The velocity for most surveyed points with annual displacement rates larger than 15 cm increased by a factor of 3–5 in summer 2008 in comparison to the winter-spring of 2007–2008. For instance, the displacement at Rastplatz around the center of the landslide rose from 12 ± 3 to 45 ± 6 cm/yr between October 2007 to May 2008 (225 days) and May 2008 to October 2008 (129 days). Considering that the velocities during the winter 2007–2008 were significantly smaller than the velocities observed by InSAR between the

Figure 3. Displacement maps of the Aletschwald landslide from satellite SAR interferometry for different sensors, time periods, and acquisition time intervals: (a) ERS SAR 19921006_19930921, (b) ENVISAT ASAR 20070629_20070803, (c) JERS SAR 19930617_19960804, (d) ALOS PALSAR. 20060613_20061029, (e) TerraSAR-X 20080822_20080913, and (f) ERS SAR 19950811_19960726. The displacement is in the line-of-sight direction, and the negative sign indicates the direction away from the satellite.

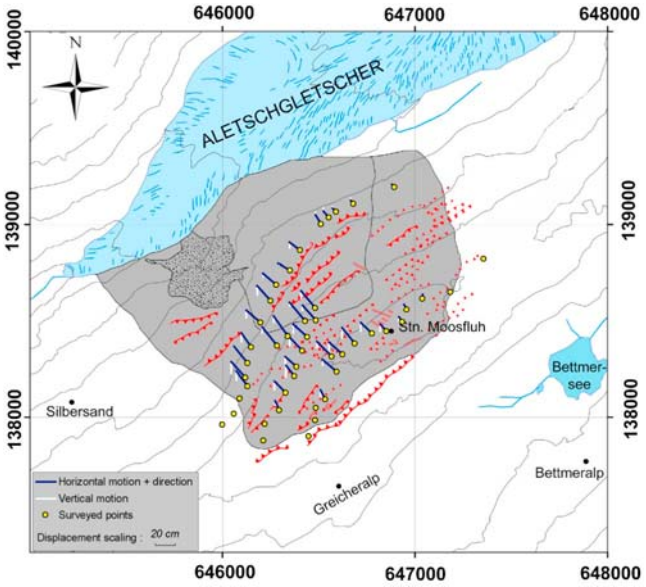

Figure 4. Differential GPS measurements of the Aletschwald landslide from 17 October 2007 to 6 October 2008, with the arrows indicating the direction and magnitude of the displacements.

summer of 2007 and 2008, we can suppose that seasonal variations of the landslide activity occur in close relationship with the refilling of the fissural groundwater reservoir by snowmelt in May–June.

3.4. Airborne Digital Photogrammetry

[25] The photogrammetric compilation of the Aletschwald unstable slope revealed no significant movement (i.e., <1 cm/yr) between 1976 and 1995. Between 1995 and 2006 a horizontal surface speed of more than 7 cm/yr was found (see Figure 5). For validation, the velocities between 1976 and 2006 were also measured. The according results were largely identical to the 1995–2006 results, confirming the almost stable conditions between 1976 and 1995. The flow direction is mainly toward the northwest and is consistent with the GPS surveys. As previously observed with the InSAR maps, the limit of the landslide is essentially sharp at the southwest of the slope and smoother toward northeast. Close to Great Aletsch Glacier, velocities could not be measured because of the presence of the glacier in 1995. In general, the significant vegetation growth between 1995 and 2006 caused some problems in the photogrammetric analysis. The according mismatches in the cross correlation between the repeat orthoimages were detected and eliminated applying a threshold for the correlation coefficient of 0.4 for measurements to be accepted.

4. Discussion

[26] In order to compare all the different displacement maps derived with various sensors and acquisition time intervals, we extracted the displacement around the center of the landslide (i.e., at Rastplatz, 138′562°N and 646′473°E) and at the end of a cableway (i.e., at Station Moosfluh, 138′456°N and 646′874°E) and transformed them to total annual displacement rates. The two plots are presented in Figures 6 and 7. In both Figures 6 and 7 the vertical error bars indicate an estimate of the displacement error, and the horizontal bars indicate the acquisition time intervals. Larger displacement rate errors are expected for shorter time intervals, in particular, for the SAR interferometric results.

[27] The compilation of the magnitude of the displacement is trivial from the DGPS surveys, being as both horizontal and vertical components of the motion are available. The displacement error has been estimated at ± 2 cm. The horizontal displacements determined with APD were transformed along the elevation gradient using the DEM, with values of 4° at Station Moosfluh and of 27° at Rastplatz. Also, the InSAR line-of-sight displacements were transformed to displacement rates along the elevation gradient using the DEM. By filtering the 25 m resolution DEM with a 625 m window, we obtained broad orientation angles with respect to the east of 144° at Station Moosfluh and of 138° at Rastplatz, which are very close to the values of 136° and 137° measured with ADP, respectively. The assumed InSAR phase error was one quarter of wavelength for ERS, Envisat, and TerraSAR-X and one eighth of wavelength for JERS and ALOS.

[28] In Figure 6 we can observe three periods of different activity, from 1992 to 1998, from 1999 to 2005, and in the last three years. The ERS/Envisat displacement rates increased from ~4 cm/yr at the beginning of the observation period to ~10 cm/yr around 2000 and to more than 30 cm/yr in the summer of 2007. These values are consistent with the rates detected with JERS, ALOS, and TerraSAR-X InSAR. The displacement values measured at the center of the landslide with DGPS in around one year are lower than those determined with InSAR with a monthly time interval. This supports the hypothesis that seasonal variations of the

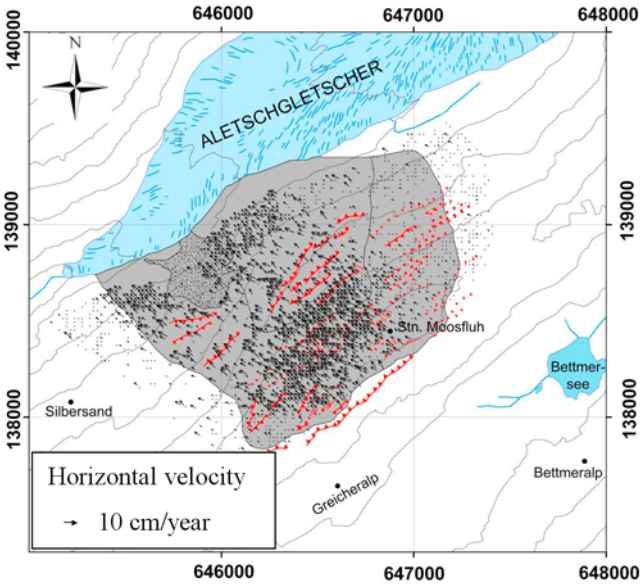

Figure 5. Digital photogrammetry measurements of the Aletschwald landslide from 2 October 1995 to 5 September 2006, with the arrows indicating the direction and magnitude of the displacements.

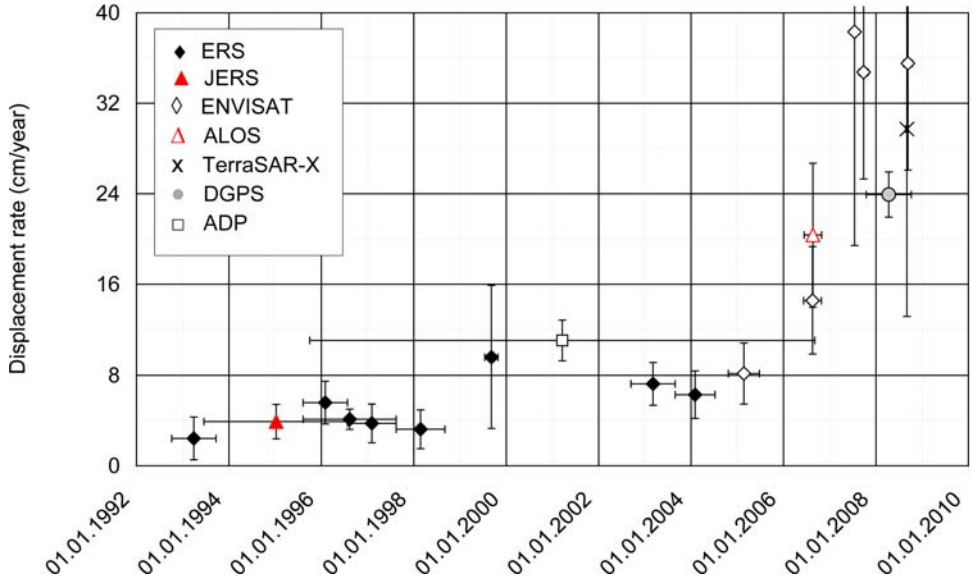

Figure 6. Magnitude of the displacement rates around the center of the landslide (Rastplatz).

landslide activity occur, with winter velocities significantly smaller than summer ones. The compilation of movement rates from ADP between 1995 and 2006 is providing a very high spatial resolution overview of the total displacement spanning the three periods of activity observed with InSAR. Because the total displacement determined with ADP between 1976 and 1995 was smaller than 1.0 cm/yr, it appears well possible that the movement of the rock mass only started to be pronounced at the beginning of the 1990s.

[29] In the summer of 1999 the increase of the displacement was possibly triggered by exceptionally strong snowfall during January and February, the corresponding large amount of meltwater in the following spring, and additional heavy spring rainfall. Indeed, in the spring of 1999 as many as 350 landslides in Switzerland were triggered with a total damage of ~40–50 Mio Euros [*Bollinger et al.*, 2000]. The summer of 2005 represented also an extraordinary period of high precipitation events in Switzerland and a large number of landslides were reported, in particular, in the central part of the country. The glaciological year 2004–2005 was also characterized by the largest retreat of Great Aletsch Glacier ever recorded, that is, 136 m (Swiss Glacier Monitoring Network, http://glaciology.ethz.ch/messnetz, accessed 15 March 2009). Both events, strong precipitation and large glacier retreat, may have contributed to the distinct acceleration of the landslide.

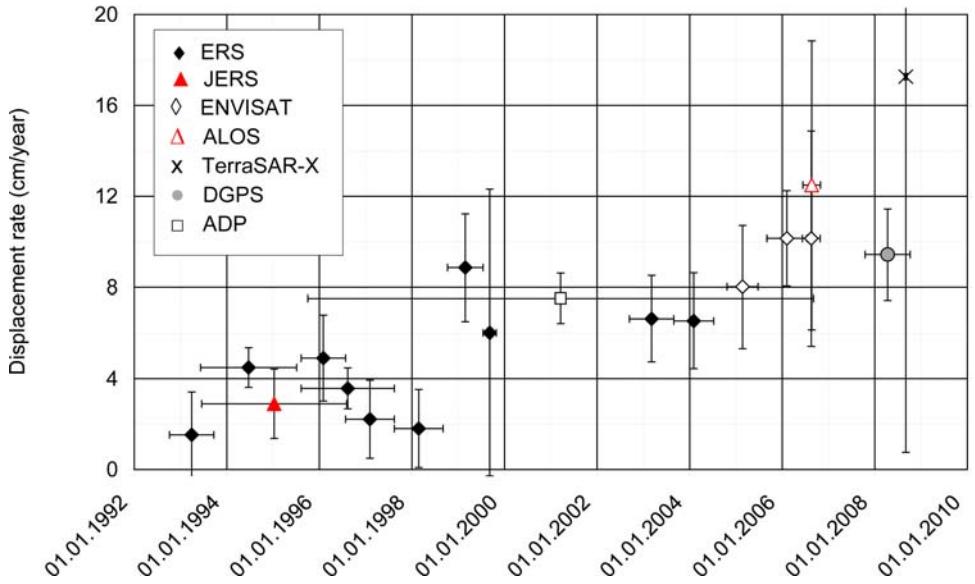

Figure 7. Magnitude of the displacement rates at the end of the cableway (Station Moosfluh).

[30] For the top station of the cableway the projection along the slope is uncertain because there the area is rather flat. Also, the error bars of some of the InSAR measurements in Figure 7 are quite large compared to the observed displacement. Therefore, the Envisat displacement rates for time intervals of less than 70 days are not presented in Figure 7. Nevertheless, the increase of the displacement rate from 1992 to 2008 is also evident here. DGPS and ADP measurements confirm the InSAR indication that the movement ongoing around the top station of the cableway is not negligible.

[31] The observed rock mass movement could have been consecutive to postglacial rebound of the slope by the end of the Last Glaciation [*Ustaszewski et al.*, 2008]. The glacial retreat caused an elastoplastic decompression and uplift [*Ambrosi and Thuering*, 2004] and probably reduction of rock mass properties and increase in fracturation by changing the stress in the upper crust [*Ustaszewski et al.*, 2008]. Numerical models studying the initialization of slope rupture on alpine slopes [*Ambrosi and Crosta*, 2006] show that under particular geological and structural conditions, the decompression is followed by continuous rock mass rupture that propagates from the toe to the crest of the slope. After completion of a rupture surface the landslide entered into a kinematic phase of potentially unstable equilibrium, moving slowly downhill and increasing the total displacement on the faults. The most evident signs of this ancient movement are the scarps in the upper part of the slope that show several meters of displacement toward northwest. However, considering that the Egesen moraine is continuous across the moving area, the displacement during the Holocene has not been substantial for long time periods, despite the glacier having been several times smaller than it is today.

[32] The significant reactivation of the quiescent landslide since the 1990s is mainly the result of continued debutressing of the valley flanks from the retreating Grosser Aletsch Glacier, which has lost in the region of interest 310 m of ice thickness since the LIA. Perhaps the ancient deep vertical scarps are also reactivated by the current decompression phase, explaining the low rate of subsidence in the upper part of the landslide. Strong precipitation and snowmelt events contributed to distinct accelerations of the movements in 1999 and 2005. A sustained displacement rate of the entire rock mass in the slope-parallel direction may contribute to catastrophic failures at the front of the landslide.

[33] Forthcoming DGPS measurements planned for the beginning and the end of the summer 2009 will give further indications about seasonal variations of the landslide activity already observed between the winter 2007–2008 and the summer 2008. Besides temporal variations of the landslide velocity, spatial difference in the displacement field was also observed, in particular, in the lower section. For instance, the displacement maps derived from Envisat InSAR in the summer of 2007 (Figure 3b) and ADP between 1995 and 2006 (Figure 5) indicate an important movement of the northwest section of the landslide. On the other hand, the displacement maps derived from JERS InSAR between 1993 and 1996 (Figure 3c) and TerraSAR-X in the summer of 2008 (Figure 3e) show in this area a rate smaller than elsewhere on the landslide. For future DGPS measurements, additional points will be surveyed at lower elevation close the glacier.

5. Conclusions

[34] We observed the displacement of an unstable slope in the Aletschwald region between 1976 and 2008 with satellite SAR interferometry from the ERS-1, JERS, ERS-2, Envisat, ALOS, and TerraSAR-X satellites, differential GPS measurements, matching of repeat airborne photographs, and airborne photography interpretation. We first applied InSAR for the detection of the unstable slope with a rough indication of the extent and velocity of the moving area [*Strozzi et al.*, 2002]. In a second step, after the disclosure of a considerable speedup of the landslide with further InSAR maps [*Strozzi et al.*, 2007], we monitored the evolution of displacement with time with DGPS and ADP in addition to InSAR.

[35] From in situ and airborne photography interpretation it appears that the landslide was activated at the end of the late glacial epoch, because the glacially eroded surface at Moosfluh is no more intact. Considering that the Egesen moraine is continuous across the moving area and that there is still no direct visible sign of the ongoing reactivation of the landslide when visiting the area, it can also be concluded that there has been no significant long-lasting activity of the landslide during the Holocene. The exponentially increasing reactivation of the landslide since the 1990s revealed with InSAR is therefore the result of debutressing of the valley flank due to the Great Aletsch Glacier retreat in combination with strong precipitation and snowmelt events. Future survey of the Aletschwald rock mass movement is possible every year with DGPS, airborne photographs that are taken annually over the tongue of Great Aletsch Glacier, and with Envisat ASAR, ALOS PALSAR, and TerraSAR-X InSAR. However, if higher temporal sampling of measurements would be required by a dramatic increase of the movement rate or a local collapse, other surveying methods should be employed, for example, extensiometers, automated total station, or terrestrial radar interferometry.

[36] The recent significant shrinking of glaciers observed for most mountain regions around the world [*Zemp et al.*, 2008] will potentially lead to an increasing number of paraglacial landslides such as the one studied here. In addition, the lower limit of the alpine permafrost seems to rise [*Frauenfelder and Kääb*, 2000; *Frauenfelder et al.*, 2001] with a further potential destabilization of slopes [*Wegmann et al.*, 1998; *Noetzli et al.*, 2003; *Fischer et al.*, 2006]. Collapsing rock glaciers showing morphological indices of landslide-like mass wasting (e.g., development of transversal cracks, surface subsidence of the upper section, and rapid advance of the front position) have been, for instance, reported recently from several regions in the European Alps [*Kääb et al.*, 2007; *Roer et al.*, 2008]. Combined use of satellite SAR interferometry, differential GPS, airborne digital photogrammetry, and airborne photography interpretation represents an efficient remote sensing survey of alpine displacements, even if these types of analyses are still time consuming and restricted to specialists in the relevant disciplines.

[37] The conclusions drawn about measurement methodology for the Aletschwald landslide can be easily exported

to other alpine areas. Altogether, InSAR, ADP, and DGPS provide different kinematic quantities that complement each other well within a hazard assessment procedure [*Kääb*, 2005; *Brückl et al.*, 2006; *Delacourt et al.*, 2007]. SAR interferometry appears to be the method of choice for a large-scale survey of slope instabilities, with the possibility in certain cases to reveal the temporal development of the line-of-sight displacement since the 1990s. Once a geological screening has been performed and potentially problematic situations have been identified, airborne photography interpretation can be used to better characterize the slope instabilities. Multitemporal ADP gives the area-wide elevation changes and horizontal displacements (or three-dimensional particle movement) and allows going further back in time, provided earlier airborne photographs are available. As a final monitoring step, terrestrial methods such as DGPS provide displacement information with high accuracy and temporal resolution but only for selected points. The combination of all these quantities allows for modeling the slide mechanisms involved in a particular mass movement.

[38] **Acknowledgments.** ERS and Envisat SAR data are courtesy of CP1.2338, copyright ESA. JERS SAR data are courtesy of J-2RI-001, copyright JAXA. ALOS PALSAR data are courtesy of P-175-001, copyright JAXA. TerraSAR-X data are courtesy of LAN0242, copyright DLR. DHM25 is copyright 2003 swisstopo. Aerial photography was reproduced by permission of swisstopo (BA081844). The work of A. Kääb is supported by the Research Council of Norway (International Centre for Geohazards SFF-ICG 146035/420 and project CORRIA 185906/V30).

References

Ambrosi, C., and G. Crosta (2006), Large sackung along major tectonic features in the Central Italian Alps, *Eng. Geol. Amsterdam*, *83*(1–3), 183–200, doi:10.1016/j.enggeo.2005.06.031.

Ambrosi, C., and M. Thuering (2004), Geotechnical modeling of large slope movements: The Cerentino landslide (Ticino, Switzerland), paper presented at Swiss Geoscience Meeting 2004: Natural hazards and mass transport in mountain ranges, Swiss Acad. of Sci., Lausanne, Switzerland, 19–20 Nov.

Ballantyne, C. (2002), Paraglacial geomorphology, *Quat. Sci. Rev.*, *21*, 1935–2017, doi:10.1016/S0277-3791(02)00005-7.

Bamler, R., and P. Hartl (1998), Synthetic aperture radar interferometry, *Inverse Probl.*, *14*, R1–R54, doi:10.1088/0266-5611/14/4/001.

Blair, R. (1994), Moraine and valley wall collapse due to rapid deglaciation in Mount Cook National Park, New Zealand, *Mt. Res. Dev.*, *14*(4), 347–358, doi:10.2307/3673731.

Bollinger, D., C. Hegg, H. R. Keusen, and O. Lateltin (2000), Ursachenanalyse der Hanginstabilitäten 1999, *Bull. Angew. Geol.*, *5*(1), 5–38.

Brückl, E., F. Brunner, and K. Kraus (2006), Kinematics of a deep-seated landslide derived from photogrammetric, GPS and geophysical data, Eng. *Geol. Amsterdam*, *88*(3–4), 149–159, doi:10.1016/j.enggeo.2006.09.004.

Catani, F., P. Farina, S. Moretti, G. Nico, and T. Strozzi (2005), On the application of SAR interferometry to geomorphological studies: Estimation of landform attributes and mass movements, *Geomorphology*, *66*(1–4), 119–131.

Crisinel, A. (1978), Geologie de la reserve naturelle de la forêt d'Aletsch (Valais-Suisse), *Bull. Murithienne*, *95*, 45–58.

Crosetto, M., O. Monserrat, C. Bremmer, R. Hanssen, R. Capes, and S. Marsh (2008), Ground motion monitoring using SAR interferometry: Quality assessment, *Eur. Geol.*, *26*, 12–15.

Delacourt, C., P. Allemand, E. Berthier, D. Raucoules, B. Casson, P. Grandjean, C. Pambrun, and E. Varel (2007), Remote-sensing techniques for analysing landslide kinematics: A review, *Bull. Soc. Geol. Fr.*, *178*(2), 89–100, doi:10.2113/gssgfbull.178.2.89.

Delaloye, R., C. Lambiel, R. Lugon, H. Raetzo, and T. Strozzi (2007), Typical ERS InSAR signature of slope movements in a periglacial mountain environment (Swiss Alps), paper presented at Envisat Symposium, Eur. Space Agency, Montreux, Switzerland, 23–27 April.

Fischer, L., A. Kääb, C. Huggel, and J. Noetzli (2006), Geology, glacier retreat and permafrost degradation as controlling factors of slope instabilities in a high-mountain rock wall: The Monte Rosa east face, *Nat. Hazards Earth Syst. Sci.*, *6*(5), 761–772.

Frauenfelder, R., and A. Kääb (2000), Towards a palaeoclimatic model of rock glacier formation in the Swiss Alps, *Ann. Glaciol.*, *31*, 281–286, doi:10.3189/172756400781820264.

Frauenfelder, R., W. Haeberli, M. Hoelzle, and M. Maisch (2001), Using relict rockglaciers in GIS-based modelling to reconstruct younger Dryas permafrost distribution patterns in the Err-Julier area, Swiss Alps, Norwegian, *J. Geog.*, *55*(4), 195–202.

Goldstein, R., and C. Werner (1997), Radar ice motion interferometry, paper presented at 3rd ERS Symposium, Eur. Space Agency, Florence, Italy.

Kääb, A. (2002), Monitoring high-mountain terrain deformation: Examples using digital aerial imagery and ASTER data, *ISPRS J. Photogramm. Remote Sens.*, *57*(1–2), 39–52, doi:10.1016/S0924−2716(02)00114−4.

Kääb, A. (2005), *Remote Sensing of Mountain Glaciers and Permafrost Creep*, *Schriftenr. Phys. Geogr.*, vol. 48, 266 pp., Univ. of Zurich, Zurich, Switzerland.

Kääb, A., and M. Vollmer (2000), Surface geometry, thickness changes and flow fields on permafrost streams: Automatic extraction by digital image analysis, *Permafrost Periglacial Processes*, *11*(4), 315–326, doi:10.1002/1099-1530(200012)11:4<315::AID-PPP365>3.0.CO;2-J.

Kääb, A., et al. (2005), Remote sensing of glacier- and permafrost-related hazards in high mountains: An overview, *Nat. Hazards Earth Syst. Sci.*, *5*(4), 527–554.

Kääb, A., R. Frauenfelder, and I. Roer (2007), On the response of rock-glacier creep to surface temperature increase, *Global Planet. Change*, *56*(1–2), 172–187, doi:10.1016/j.gloplacha.2006.07.005.

Kaufmann, V., and R. Ladstädter (2000), Spatio-temporal analysis of the dynamic behavior of the Hochebenkar rock glaciers (Oetztal Alps, Austria) by means of digital photogrammetric methods, paper presented at 6th International Symposium on High Mountain Remote Sensing Cartography, High Mt. Remote Sens. Cartogr. Soc., Ethiopia.

Kelly, M., P. Kubik, F. von Blanckenburg, and C. Schlüchter (2004), Surface exposure dating of the Great Aletsch Glacier Egesen moraine system, western Swiss Alps, using the cosmogenic nuclide ^{10}Be, *J. Quat. Sci.*, *19*(5), 431–441, doi:10.1002/jqs.854.

Lambiel, C., and R. Delaloye (2004), Contribution of real-time kinematic GPS in the study of creeping mountain permafrost: Examples from the Western Swiss Alps, *Permafrost Periglacial Processes*, *15*, 229–241, doi:10.1002/ppp.496.

Matsuoka, N., and A. Masahiro (2002), Rock slope failures associated with deglaciation: Some examples from glaciated valleys in the Swiss Alps, *Annu. Rep. 28*, pp. 11–16, Inst. of Geosci., Univ. of Tsukuba, Tsukuba, Japan.

Noetzli, J., M. Hoelzle, and W. Haeberli (2003), Mountain permafrost and recent Alpine rock-fall events: A GIS-based approach to determine critical factors, paper presented at 8th International Conference on Permafrost, Int. Permafrost Assoc., Zurich, Switzerland.

Paul, F., and W. Haeberli (2008), Spatial variability of glacier elevation changes in the Swiss Alps obtained from two digital elevation models, *Geophys. Res. Lett.*, *35*, L21502, doi:10.1029/2008GL034718.

Paul, F., A. Kääb, M. Maisch, T. Kellenberger, and W. Haeberli (2004), Rapid disintegration of Alpine glaciers observed with satellite data, *Geophys. Res. Lett.*, *31*, L21402, doi:10.1029/2004GL020816.

Roer, I., M. Avian, R. Delaloye, C. Lambiel, W. Haeberli, A. Kääb, and V. Kaufmann (2008), Observations and considerations on collapsing active rockglaciers in the Alps, paper presented at Ninth International Conference on Permafrost, Int. Permafrost Assoc., Fairbanks, Alaska, July.

Rosen, P., S. Hensley, I. Joughin, F. Li, S. Madsen, E. Rodriguez, and R. Goldstein (2000), Synthetic aperture radar interferometry, *Proc. IEEE*, *88*(3), 333–382, doi:10.1109/5.838084.

Sandwell, D., D. Myer, R. Mellors, M. Shimada, B. Brooks, and J. Foster (2008), Accuracy and resolution of ALOS interferometry: Vector deformation maps of the Father's day intrusion at Kilauea, *IEEE Trans. Geosci. Remote Sens.*, *46*(11), 3524–3534, doi:10.1109/TGRS.2008.2000634.

Strozzi, T., U. Wegmüller, L. Tosi, G. Bitelli, and V. Spreckels (2001), Land subsidence monitoring with differential SAR interferometry, *Photogramm. Eng. Remote Sens.*, *67*(11), 1261–1270.

Strozzi, T., U. Wegmüller, C. Werner, and A. Wiesmann (2002), Alpine landslide periodical survey, paper presented at International Geoscience and Remote Sensing Symposium 2002, Int. Electr. and Electron. Eng., Toronto, Canada, 24–28 June.

Strozzi, T., A. Kääb, R. Frauenfelder, and U. Wegmüller (2003), Detection and monitoring of unstable high-mountain slopes with L-band SAR interferometry, paper presented at International Geoscience and

Remote Sensing Symposium 2003, Int. Electr. and Electron. Eng., Toulouse, France, 21–25 July.

Strozzi, T., A. Kääb, and R. Frauenfelder (2004), Detecting and quantifying mountain permafrost creep from in situ inventory, space-borne radar interferometry and airborne digital photogrammetry, *Int. J. Remote Sens.*, *25*(15), 2919–2931, doi:10.1080/0143116042000192330.

Strozzi, T., P. Farina, A. Corsini, C. Ambrosi, M. Thüring, J. Zilger, A. Wiesmann, U. Wegmüller, and C. Werner (2005), Survey and monitoring of landslide displacements by means of L-band satellite SAR interferometry, *Landslides*, *2*(3), 193–201, doi:10.1007/s10346-005-0003-2.

Strozzi, T., U. Wegmüller, E. Perruchoud, R. Delaloye, A. Kääb, and C. Ambrosi (2007), Evolution of a deep-seated rock mass movement observed with satellite SAR interferometry, paper presented at Fringe 2007 Workshop, Eur. Space Agency, Frascati, Italy, 26–30 Nov.

Ustaszewski, M., A. Hampel, and A. Pfiffner (2008), Composite faults in the Swiss Alps formed by the interplay of tectonics, gravitation and postglacial rebound: An integrated field and modelling study, *Swiss J. Geosci.*, *101*, 223–235, doi:10.1007/s00015-008-1249-1.

Wegmann, M., G. H. Gudmundsson, and W. Haeberli (1998), Permafrost changes in rock walls and the retreat of alpine glaciers: A thermal modelling approach, *Permafrost Periglacial Processes*, *9*(1), 23–33, doi:10.1002/(SICI)1099-1530(199801/03)9:1<23::AID-PPP274>3.0.CO;2-Y.

Werner, C., U. Wegmüller, T. Strozzi, and A. Wiesmann (2002), Processing strategies for phase unwrapping for INSAR applications, paper presented at European Conference on Synthetic Aperture Radar: EUSAR 2002, Verband der Elektrotech. Elektron. Informationstechnik, Cologne, Germany, 4–6 June.

Zemp, M., I. Roer, A. Kääb, M. Hoelzle, F. Paul, and W. Haeberli (2008), Global glacier changes: Facts and figures, report, 88 pp., U. N. Environ. Programme and World Glacier Monit. Serv., Geneva, Switzerland.

C. Ambrosi, Institute of Earth Sciences, University of Applied Sciences of Southern Switzerland, PO Box 72, CH-6952 Canobbio, Switzerland.

R. Delaloye and E. Perruchoud, Geography Unit, Department of Geosciences, University of Fribourg, Ch. du Musée 4, CH-1700 Fribourg, Switzerland.

A. Kääb, Department of Geosciences, University of Oslo, PO Box 1047, Blindern, N-0316 Oslo, Norway.

T. Strozzi and U. Wegmüller, Gamma Remote Sensing, Worbstrasse 225, CH-3073 Gümligen, Switzerland. (strozzi@gamma-rs.ch)